The instability of streaks in near-wall turbulence

By G. Kawahara, J. Jiménez, M. Uhlmann[1] AND A. Pinelli[1]

1. Motivation and objectives

Several aspects of the self-sustaining mechanism of near-wall turbulence have been studied recently (see Jiménez & Moin 1991; Hamilton, Kim & Waleffe 1995; Waleffe 1997; Schoppa & Hussain 1997; Jiménez & Pinelli 1998). It is well-known that there are two key structures, streamwise vortices and streaks, in the near-wall region. Streamwise vortices generate streaks through the deformation of the mean flow by their induced cross-flow advection. The streaks, which are nearly uniform in the streamwise direction, become unstable, bending along the streamwise direction and leading to the production of streamwise vorticity. Finally, the produced streamwise vorticity evolves nonlinearly into streamwise vortices. In this manner streamwise vortices and streaks generate each other sequentially to sustain near-wall turbulence.

The instability of streaks, to be discussed in this report, is expected to be a crucial ingredient in the self-sustaining cycle. If the streaks were not unstable, then the streamwise vortices should decay under the action of viscosity and so also should the streaks. This decay would mean a termination of the regeneration cycle. Therefore, controlling the streak instability could reduce drag or enhance heat and momentum transfer in near-wall turbulent flows. The control of streaks seems to be easier than that of streamwise vortices since streaks have much larger length scale in the streamwise direction compared to that of streamwise vortices. Because streaky flows over a wall depend on the spanwise direction as well as the wall-normal direction, we cannot apply Squire's transformation to the streak instability, and thus we must consider the three-dimensional mechanism for the instability.

Waleffe (1995, 1997) and Waleffe & Kim (1997) examined numerically the linear stability of streaks in a plane Couette flow at a low Reynolds number. They employed the streamwise velocity field deformed by assumed streamwise rolls as a base flow to demonstrate that sinuous modes, which have often been observed experimentally and numerically, actually grow via the instability mechanism. They stated that the instability originates from inflection points, i.e. wake-like instability, in the spanwise variation of streaky flows. Reddy *et al.* (1998) investigated the same instability systematically in plane Poiseuille flow as well as in plane Couette flow to study subcritical transition. For a turbulent channel flow, on the other hand, Schoppa & Hussain (1997, 1998) examined the time-evolution of small disturbances embedded in a model flow for streaks (on only one wall) by using direct numerical simulations. They found an exponential growth of sinuous modes and discussed the mechanism of the instability. They remarked that the streak instability is not the

1 The School of Aeronautics, U. Politécnica Madrid

same as the wake-like instability; rather, it is similar to the oblique instability of a shear layer. However, at least in the initial linear phase, the structure of growing disturbances which Schoppa & Hussain (1998) observed in their turbulent channel flow is similar to that in a plane Couette flow where the streak instability has been considered to be the same as the wake-like instability, as mentioned above. Much effort has been devoted to investigating the streak instability, but we must admit that our knowledge is still poor concerning the mechanism and the structure of the instability.

The main objectives of our present work are to elucidate the conditions for the streak instability in a turbulent channel flow and to demonstrate the generation mechanism of the streamwise vorticity through the streak instability. We expect that the understanding of the conditions and the streamwise vorticity generation in the streak instability could provide useful information for turbulence control in near-wall flows. In order to accomplish these objectives, we have performed numerically the linear stability analysis of a turbulent-channel-type base flow with a periodic undulation in the spanwise direction.

2. Accomplishments

2.1 Base flow

In the following linear stability analysis, x, y, and z are used to represent the streamwise, the wall-normal, and the spanwise coordinates, respectively. Friction velocity u_τ and channel half-width h (and a resulting time scale h/u_τ) are taken as reference velocity and length (and reference time) for non-dimensionalization.

The base flow to be considered here is a unidirectional flow and has only the x-component of dimensionless velocity, U. U is dependent on both y- and z-coordinates as

$$U(y,z) = U_0(y) + U_1(y)\cos(\gamma z), \tag{1}$$

where $U_0(y)$ stands for a typical mean velocity profile of a turbulent channel flow and is given by numerical integration of (see Reynolds & Tiederman 1967)

$$\frac{\mathrm{d}U}{\mathrm{d}y} = -\frac{Re_\tau(y-1)}{1+\nu_t(y-1)} \quad (0<y<2). \tag{2}$$

The function $\nu_t(\xi)$ is expressed as

$$\nu_t(\xi) = \frac{1}{2}\left\{1+\left[\frac{KRe_\tau}{3}(1-\xi^2)(1+2\xi^2)\left(1-\exp\left(-\frac{Re_\tau(1-|\xi|)}{A}\right)\right)\right]^2\right\}^{\frac{1}{2}} - \frac{1}{2}. \tag{3}$$

Here

$$Re_\tau = \frac{u_\tau h}{\nu} \tag{4}$$

is a Reynolds number, and ν is the kinematic viscosity of the fluid. In this work we restrict ourselves to a low-Reynolds-number turbulent channel flow by setting

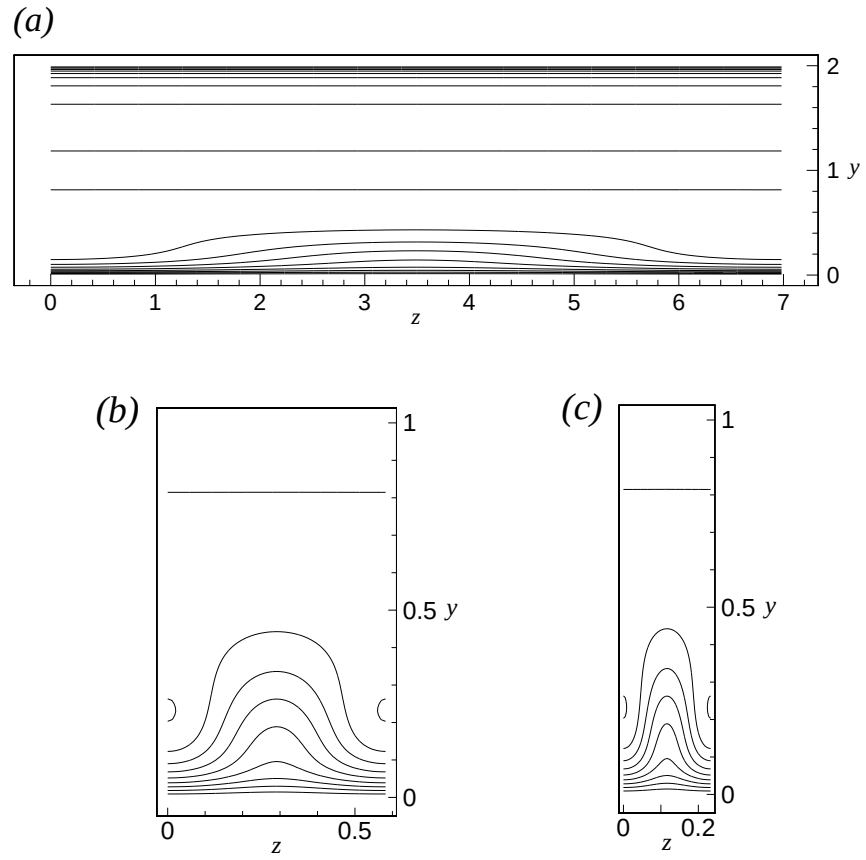

FIGURE 1. Contour plot on (y, z)-plane of the streamwise velocity of the base flow (1) for (a) $\Delta U = 3.0$, $\gamma = 0.9$; (b) $\Delta U = 4.0$, $\gamma = 10.8$; and (c) $\Delta U = 4.0$, $\gamma = 27.0$. Contour increment is 2. Only half the height of the channel is shown in (b) and (c). Modes I, II and III in Fig. 4 have been obtained respectively for the base flows (a), (b), and (c).

$Re_\tau = 180$. In this case the value of the Reynolds number based on the channel centerline velocity is 3300. We have set the values of the adjustable parameters in (3) as $K = 0.525$, $A = 37$ so that the velocity profile $U_0(y)$ can fit a realistic profile for $Re_\tau = 180$ (Waleffe, Kim & Hamilton 1991). On the right-hand side of (1) the second term represents low- and high-speed streaks alternating in the spanwise direction with dimensionless wavenumber γ. $U_1(y)$ is the dimensionless amplitude of the spanwise variation given by

$$U_1(y) = \Delta U \frac{\sqrt{\sigma} y \exp(-\sigma y^2)}{\exp(-1/2)/\sqrt{2}}, \tag{5}$$

which has a maximum ΔU at $y = (2\sigma)^{-1/2}$ and is localized on the lower wall $y = 0$. Here, we set $\sigma = 18$ so that the maximum streak velocity (and so the maximum wall-normal vorticity $\gamma \Delta U$) may be located at $y = \frac{1}{6}$, i.e. 30 wall units. Figure 1

shows the contour plot on (y, z)-plane of the streamwise velocity for the three typical base flows to be discussed in §§2.4 and 2.5.

We confirmed that the y-dependence (5) of streaky flows approximately represents that of real streaks in comparison to the streamwise velocity fluctuation in direct numerical simulations. A similar type of streaks to (5) was also used in Schoppa & Hussain (1997, 1998).

We should note that the base flow (1) is not an exact solution to the Navier-Stokes equation and the actually observed streaky flows have weak time- and x-dependence. However, we believe that the base flow (1) is valid as the first step of the analysis because real near-wall streaks have much larger time and streamwise length scales than those of typical turbulence structures, e.g. streamwise vortices. Another possibility is to obtain fully nonlinear equilibrium solutions, which correspond to streaky flows, in some moving reference frame. But this lies outside the scope of the present work. As is well known, the turbulent-channel-type base flow $U_0(y)$ alone does not possess any unstable eigenmodes of the linearized Navier-Stokes equation.

2.2 Linear stability analysis

When we consider the linear stability problem for the base flow (1), we cannot use Squire's transformation, and thus we must consider three-dimensional disturbances. If wall-normal disturbance velocity v and vorticity η are taken as dependent variables, the time-evolution of an infinitesimal disturbance may be described by the extended Orr-Sommerfeld equation

$$\left(\partial_t + U\partial_x - \frac{1}{Re_\tau}\nabla^2\right)\nabla^2 v - \left[\left(\partial_y^2 - \partial_z^2\right)U\right]\partial_x v \\ -2\left(\partial_z U\right)\partial_x\left(\partial_y w - \partial_z v\right) - 2\left(\partial_y\partial_z U\right)\partial_x w = 0, \qquad (6)$$

and by the extended Squire equation

$$\left(\partial_t + U\partial_x - \frac{1}{Re_\tau}\nabla^2\right)\eta - \left(\partial_z U\right)\partial_y v + \left(\partial_y U\right)\partial_z v + \left(\partial_y\partial_z U\right)v + \left(\partial_z^2 U\right)w = 0 \quad (7)$$

(see Waleffe 1995), where spanwise disturbance velocity w is related to v and η as

$$\left(\partial_x^2 + \partial_z^2\right)w = -\partial_y\partial_z v - \partial_x\eta. \qquad (8)$$

We have used the continuity equation $\partial_x u + \partial_y v + \partial_z w = 0$ and the definition of the wall-normal vorticity $\eta = \partial_z u - \partial_x w$ to have (8), where u is the streamwise disturbance velocity. Equations (6) and (7) are supplemented by boundary conditions

$$v = \partial_y v = 0, \quad \eta = 0$$

at $y = 0$, 2.

In the following, we shall seek solutions to a system of equations (6), (7), and (8) in the normal-mode form

$$v = \mathrm{Re}\left[\hat{v}(y, z)\,\mathrm{e}^{\mathrm{i}\alpha(x-ct)}\right], \qquad (9)$$

$$\eta = \mathrm{Re}\left[\hat{\eta}(y,z)\,\mathrm{e}^{\mathrm{i}\alpha(x-ct)}\right], \tag{10}$$

$$w = \mathrm{Re}\left[\hat{w}(y,z)\,\mathrm{e}^{\mathrm{i}\alpha(x-ct)}\right], \tag{11}$$

where α stands for the streamwise wavenumber and c the complex phase velocity. The growth rate of the disturbance is given by $\alpha\mathrm{Im}(c)$.

We anticipate periodic solutions in the spanwise direction (Floquet theory). Two fundamental modes are considered, i.e. the sinuous mode

$$\hat{v} = \sum_{n=1}^{\infty} \hat{v}_n(y)\,\sin(n\gamma z), \quad \hat{\eta} = \sum_{n=0}^{\infty} \hat{\eta}_n(y)\,\cos(n\gamma z), \quad \hat{w} = \sum_{n=0}^{\infty} \hat{w}_n(y)\,\cos(n\gamma z), \tag{12}$$

and the varicose mode

$$\hat{v} = \sum_{n=0}^{\infty} \hat{v}_n(y)\,\cos(n\gamma z), \quad \hat{\eta} = \sum_{n=1}^{\infty} \hat{\eta}_n(y)\,\sin(n\gamma z), \quad \hat{w} = \sum_{n=1}^{\infty} \hat{w}_n(y)\,\sin(n\gamma z), \tag{13}$$

which are treated separately except for the case where both modes have the same eigenvalue c, since the anti-symmetric and the symmetric modes can be decoupled in (6), (7), and (8).

In the numerical solution of the eigenvalue problem, the infinite series in (12) and (13) are replaced by truncated series up to $n = N_z$ in the spanwise direction z. We then apply a Galerkin method to Eqs. (6) and (7) by using N_s b-splines of order 6 as expansion functions in the wall-normal direction y. We set $N_z = 10$ and $N_s = 40$ to have convergence under 0.2% difference for N_z and under 4% difference for N_s. More details about the discretization can be found in Jiménez *et al.* (1998). The evaluation of the involved integrals leads to a large, coupled system of algebraic equations, $\boldsymbol{A}\hat{\boldsymbol{x}} = c\boldsymbol{B}\hat{\boldsymbol{x}}$, which is of order $N_s \times (2N_z + 1)$, where $\hat{\boldsymbol{x}}$ is the solution vector in spline space and contains the coefficients of the wall-normal velocity and vorticity for each spanwise mode and each discrete wall-normal location. The algebraic eigenvalue problem was solved by using standard library routines (e.g. LAPACK or EISPACK). We have removed spurious eigenvalues that might be caused by the boundary treatment through the tau method before seeking the most unstable (or least stable) eigenvalue and eigenvector.

2.3 Neutral curves

Figure 2 shows the projection on $(\gamma, \Delta U)$-plane of the lower bound of the neutral surface in $(\gamma, \Delta U, \alpha)$-space. Open and closed circles represent the sinuous and the varicose modes, respectively. The streaky flow should be unstable above the neutral curve around the critical streamwise wavenumber α_c. Note that the corresponding spanwise wavenumber of 100 wall units is located at $\gamma/Re_\tau = 0.06$ in this figure. The critical streak amplitude ΔU_c seems to have a finite value (≈ 1.7) as $\gamma \to 0$ both for the sinuous modes and for the varicose modes.

In the case of the sinuous modes, ΔU_c increases abruptly at $\gamma/Re_\tau < 0.01$ and takes a maximum around $\gamma/Re_\tau = 0.03$. From there ΔU_c decreases with increasing

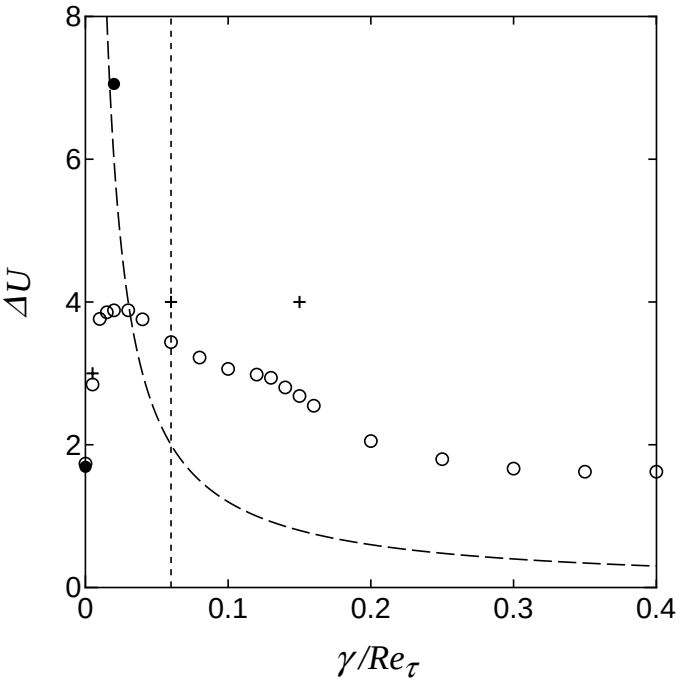

FIGURE 2. Trace of the neutral curve on $(\gamma, \Delta U)$-plane. Open circles represent the sinuous mode and closed circles represent the varicose mode. The dotted vertical line indicates $\gamma/Re_\tau = 0.06$, on which the wall-normal shear and the spanwise shear due to streaks are comparable. The dashed curve denotes the contour of a constant amplitude $\gamma\Delta U/Re_\tau = 0.12$ of the wall-normal vorticity, on which the mean shear at $y = \frac{1}{6}$ is comparable to the spanwise shear of streaks. Three crosses represent modes I, II, and III in Fig. 4.

γ. In general, the actual value of the growth rate $\alpha\mathrm{Im}(c)$ (not shown here) is increased when γ as well as ΔU are increased because they are related to the intensity of the shear layer generated by the streaks. For large γ, however, the effect of viscosity progressively stabilizes the flow. In the case of a two-dimensional wake, the critical Reynolds number is given by $Re_c \approx 5$, and in our case it is estimated as $Re_c = 2\pi Re_\tau(\Delta U/\gamma)$ (≈ 5). This estimate tells us that the stabilization due to the viscosity becomes important only for relatively large γ ($\gamma/Re_\tau \approx 1.3\Delta U$).

At $\gamma/Re_\tau = 0.06$, i.e. 100 wall-unit wavelength, the instability requires that $\Delta U > 3.44$ for the streamwise velocity and so $\gamma\Delta U/Re_\tau = 0.20$ for the wall-normal vorticity. If we take into consideration that the RMS value of the streamwise fluctuation velocity (and the wall-normal vorticity) attains the maximum of about $2.7u_\tau$ (and $0.2u_\tau^2/\nu$) in the near-wall region, then the above requirements for the instability are expected to be satisfied in a turbulent channel flow.

In the case of the varicose modes, on the other hand, ΔU_c increases abruptly with increasing γ so that a stable region is extended to almost all the parameter plane in Fig. 2.

This significant difference of the instability between the sinuous (bending) and the varicose modes could explain, at least for low Re_τ, the fact that the actually

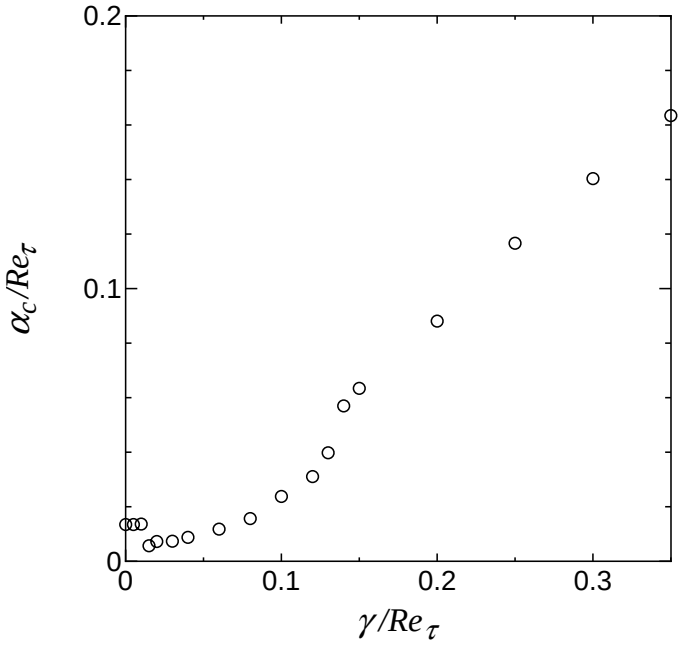

FIGURE 3. Plot of the critical streamwise wavenumber α_c against γ.

observed streak instability involves the bending motion of streaks in the spanwise direction (see Hamilton, Kim & Waleffe 1995; Schoppa & Hussain 1997; Jiménez & Pinelli 1998).

Figure 3 shows the critical streamwise wavenumber α_c against the spanwise wavenumber γ for the sinuous modes. For $\gamma/Re_\tau < 0.01$, α_c is independent of γ, taking a constant value of $\alpha_c/Re_\tau = 0.013$. At $\gamma/Re_\tau > 0.01$, α_c jumps down and gradually increases with increasing γ. For $\gamma/Re_\tau = 0.06$, i.e. 100 wall-unit wavelength, the streamwise wavenumber has a value of $\alpha_c/Re_\tau = 0.012$, which corresponds to 500 wall-unit wavelength. This wavelength is consistent with that of the streak bending often observed in a turbulent channel flow. α_c kinks at $\gamma/Re_\tau \approx 0.12$, and then α_c increases nearly linearly with γ. This jump and kink of α_c implies that there are different instability mechanisms in three ranges: $\gamma/Re_\tau < 0.01$, $0.01 < \gamma/Re_\tau < 0.12$, and $\gamma/Re_\tau > 0.12$. We can now see the corresponding dependence of ΔU_c on γ in each range of γ in Fig. 2.

In the present configuration, streaks (the second term in (1)) have the width $2\pi h/\gamma$ and the height $0.6h$ within which the (dimensionless) streak velocity exceeds $0.01\Delta U$. If $\gamma/Re_\tau = 0.06$, then the width is comparable to the height. Two time scales based on shearing motion of streaks across the spanwise and the wall-normal directions are also comparable at $\gamma/Re_\tau = 0.06$ since they should be estimated as each length scale divided by $\Delta U u_\tau$. On the other hand, the mean flow part $U_0(y)$ in (1) has the velocity gradient of $0.12Re_\tau u_\tau/h$ at $y = \frac{1}{6}$, i.e. 30 wall units, where the streak velocity and vorticity attain a maximum. Thus, at least in the vicinity of this maximum, the time scale of shearing motion of streaks across the spanwise direction is comparable to that of the mean shear if $\gamma\Delta U/Re_\tau = 0.12$.

In Fig. 2, we have shown these relations, $\gamma/Re_\tau = 0.06$ and $\gamma\Delta U/Re_\tau = 0.12$,

respectively by the dotted line and the dashed curve. It turns out that in the case of the instability at $\gamma/Re_\tau < 0.01$, the width of streaks is larger than the height and also the spanwise shear of streaks is weaker than the wall-normal shear and the mean shear. Because α_c is independent of γ for $\gamma/Re_\tau < 0.01$ as shown in Fig. 3, the spanwise shear actually does not affect the instability. In the case of the instability at $\gamma/Re_\tau > 0.12$, on the other hand, the height of streaks is larger than the width, and also the spanwise shear of streaks is stronger than the wall-normal shear and the mean shear. At $0.01 < \gamma/Re_\tau < 0.12$, where the typical streak spacing $\gamma/Re_\tau = 0.06$, i.e. 100 wall units, is located, the streak width and height as well as the streak wall-normal and spanwise shear and the mean shear are nearly comparable.

Reddy *et al.* (1998) examined numerically streak instability in the simplified model for a plane Couette flow and showed that mean shear has the stabilizing effect on the instability (see also Waleffe 1997). Baggett (1996) argued that the spanwise shear by streaks exceeds mean shear leading to the instability of streaks.

2.4 Eigenmodes

In this subsection, we shall discuss the structures of the unstable sinuous eigenmodes near the neutral surface in order to distinguish the effects of the above-mentioned different shear components on the instability.

Figure 4 shows the iso-surface of the streamwise disturbance vorticity of three unstable eigenmodes for (a) $\Delta U = 3.0$, $\gamma/Re_\tau = 0.005$, $\alpha/Re_\tau = 0.013$; (b) $\Delta U = 4.0$, $\gamma/Re_\tau = 0.06$, $\alpha/Re_\tau = 0.012$; and (c) $\Delta U = 4.0$, $\gamma/Re_\tau = 0.15$, $\alpha/Re_\tau = 0.063$ (see Fig. 1 for contour plots of the corresponding base flows). The value of the iso-surfaces is $\pm 4\omega'$, where ω' denotes the RMS value of the disturbance vorticity vector. The light gray and the dark gray iso-surfaces indicate the positive and the negative vorticity, respectively. Hereafter, the eigenmodes (a), (b), and (c) in Fig. 4 are referred to as mode I, mode II, and mode III, respectively. Modes I, II, and III have growth rates of $\alpha \mathrm{Im}(c) = 0.027$, 0.60, and 5.2 and propagate in the streamwise direction at phase velocities of $\mathrm{Re}(c) = 17.4$, 13.6, and 14.2, respectively. For all modes I, II, and III, the magnitude of the wall-normal vorticity is quite small compared to that of the other components. For mode I, the streamwise and the spanwise vorticity are comparable, while for modes II and III, the streamwise vorticity is dominant. The trace of critical points (thin curves), at which the base flow velocity is equal to $\mathrm{Re}(c)$, and of inflection points (thick curves) is shown for modes I, II, and III in Fig. 5. In this figure inflection points are defined as a point at which $\partial_n^2 U = 0$, where n is taken to be normal to iso-velocity lines (see Fig. 1) of the base flow on (y, z)-plane.

In Fig. 4, it can be seen that the three eigenmodes have strikingly different structures. In the case of mode I, the streamwise vorticity is highly localized above the high-speed streak (along the edge of the periodic box). It can be found in Fig. 5a that the critical points nearly coincide with the (upper) inflection points only above the high-speed streak. In this case the spanwise shear of the base flow is weak and inactive (see §2.3 and Fig. 2). Therefore, the instability should be characterized by the three-dimensional instability of a roughly two-dimensional wall jet.

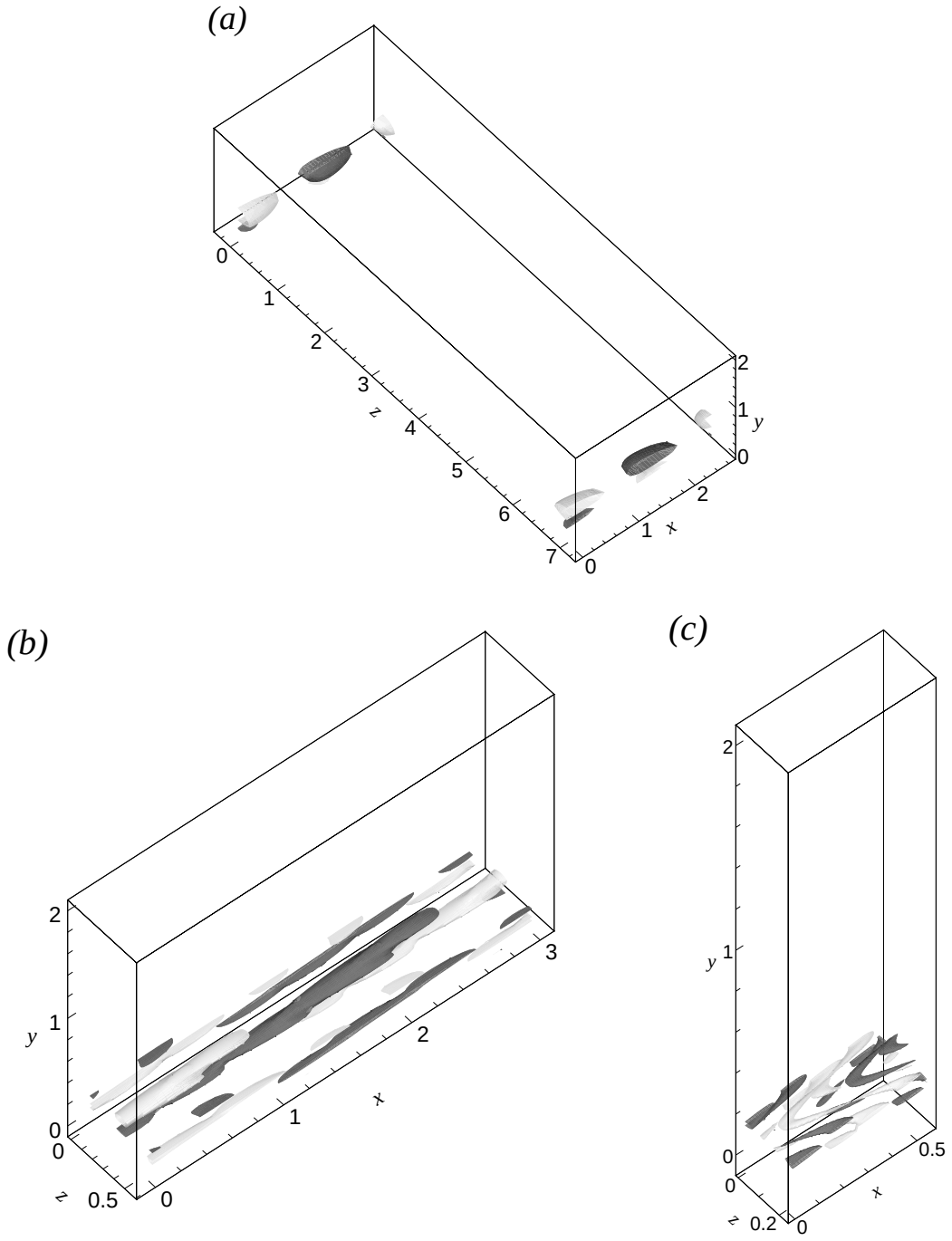

FIGURE 4. Iso-surface of the streamwise disturbance vorticity for unstable sinuous eigenmodes. (a) $\Delta U = 3.0$, $\gamma = 0.9$, $\alpha = 2.4$ (mode I); (b) $\Delta U = 4.0$, $\gamma = 10.8$, $\alpha = 2.1$ (mode II); and (c) $\Delta U = 4.0$, $\gamma = 27.0$, $\alpha = 11.4$ (mode III). The value of iso-surfaces is $\pm 4\omega'$, where ω' denotes the RMS value of the vorticity vector. The light and dark gray surfaces represent the positive and the negative vorticity. The flow is from the lower left to the upper right, and the low-speed (high-speed) streak is located along the center (edge) of the periodic box. See Fig. 1 for the corresponding base flows.

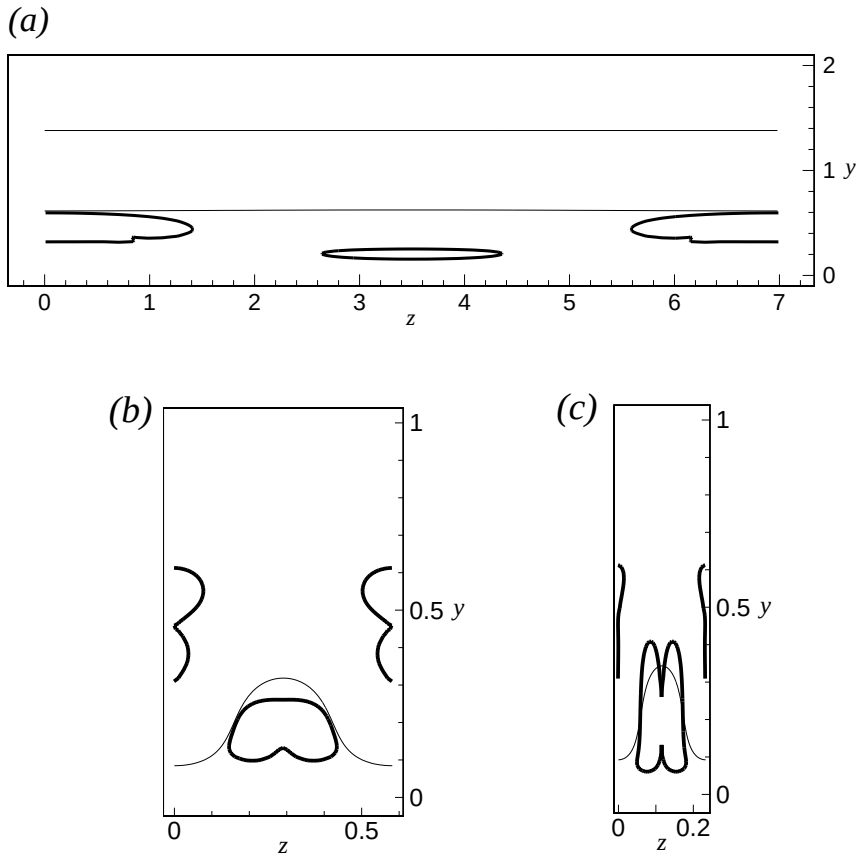

FIGURE 5. Trace of critical points and of inflection points on (y, z)-plane. (a) $\Delta U = 3.0$, $\gamma = 0.9$ (mode I); (b) $\Delta U = 4.0$, $\gamma = 10.8$ (mode II); and (c) $\Delta U = 4.0$, $\gamma = 27.0$ (mode III). The thin curves represent a critical point. The phase velocity of disturbances is $\mathrm{Re}(c) = 17.4$ for (a), $\mathrm{Re}(c) = 13.6$ for (b), and $\mathrm{Re}(c) = 14.2$ for (c). The thick curves represent a inflection point of the base flows (a), (b), and (c) in Fig. 1. Only half the height of the channel is shown in (b) and (c).

In the case of mode II, the streamwise vorticity takes an elongated ribbon-like form in the streamwise direction (Fig. 4b). The ribbon-like structures are located on both the high-speed streak and the low-speed streak (along the center of the periodic box). They are inclined in the streamwise direction from the wall-normal direction. In the case of mode III, on the other hand, the structures of the streamwise vorticity are inclined in the streamwise direction from the spanwise direction rather than from the wall-normal direction (Fig 4c). Structures of the same sign above the low- and high-speed streaks are linked via the thin 'arms' such that they appear v-shaped. This difference in the inclination direction between modes II and III could be related to the difference in the effective shear. In the case of mode III, the spanwise shear of streaks is strongest (see §2.3 and Fig. 2), so that the shearing motion across the spanwise direction could tilt eigenstructures towards the streamwise direction

from the spanwise direction. In the case of mode II, the shearing motion across the wall-normal direction is considered to be effective.

Since for both modes II and III the critical points nearly coincide with the inflection points on the flanks of the low-speed streak (Fig. 5b and c), the origin of the instability for both modes is considered to be similar to a wake instability as pointed out by Waleffe (1995, 1997) and Waleffe & Kim (1997).

In the next subsection, we examine the production of the streamwise vorticity in order to further understand the difference between modes II and III.

2.5 Production of streamwise vorticity

First, we consider the equation for the unstable modal streamwise vorticity as

$$(U-c)\,\hat{\omega}_x = -\hat{w}\,\partial_y U + \hat{v}\,\partial_z U, \tag{14}$$

or equivalently

$$\hat{\omega}_x + \mathrm{i}\frac{(U-\mathrm{Re}(c))}{\mathrm{Im}(c)}\,\hat{\omega}_x = -\mathrm{i}\frac{\hat{w}}{\mathrm{Im}(c)}\partial_y U + \mathrm{i}\frac{\hat{v}}{\mathrm{Im}(c)}\partial_z U, \tag{15}$$

where $\hat{\omega}_x(y,z)$ is related to the streamwise vorticity ω_x by $\omega_x = \mathrm{Re}\left[\hat{\omega}_x \mathrm{e}^{\mathrm{i}\alpha(x-ct)}\right]$, and we have neglected the viscous term. The right-hand side of (14) (or (15)) is responsible for the production of the streamwise vorticity through the vortex tilting. The first term in (14) (or (15)) comes from the tilting of the wall-normal disturbance vorticity by the wall-normal shear of the base flow while the second is related to the tilting of the spanwise disturbance vorticity by the spanwise shear. Note that the tilting effects of the base flow vorticity by the disturbance have disappeared from (14) (and so (15)) due to cancellation. If we estimate the order of the first and second terms for mode II and mode III, then we find that in the case of mode II the first term is significant while in the case of mode III the second is significant. The contour plots of $\hat{\omega}_x$ and of the significant production term are shown for mode II and mode III in Figs. 6 and 7, respectively (only the real parts are shown). In these figures, the flow condition of (a) corresponds to (b) in Fig. 4, and that of (b) corresponds to (c) in Fig. 4. In Fig. 7a the first term in (15) is shown, while in Fig. 7b the second term in (15) is shown.

As described in §2.4, in the case of mode II the ribbon-like structures of the positive and negative streamwise vorticity are inclined in the streamwise direction so that the positive and the negative structures are stacked alternately on top of low- and high-speed streaks (see Fig. 6a). This typical distribution of the positive and negative vorticity coincides well with that of the significant production term (Fig. 7a). In their direct numerical simulation, Sendstad & Moin (1992) found that the same production term, $-(\partial_x w)(\partial_y u)$, is dominant for the generation of the streamwise vorticity in near-wall turbulence.

For mode II, if we estimate the order of each component of the disturbance velocity, it turns out that the spanwise disturbance velocity is much larger than the wall-normal one, especially on the low- and high-speed streaks (the streamwise component is very small). The strong spanwise velocity could be induced by spanwise

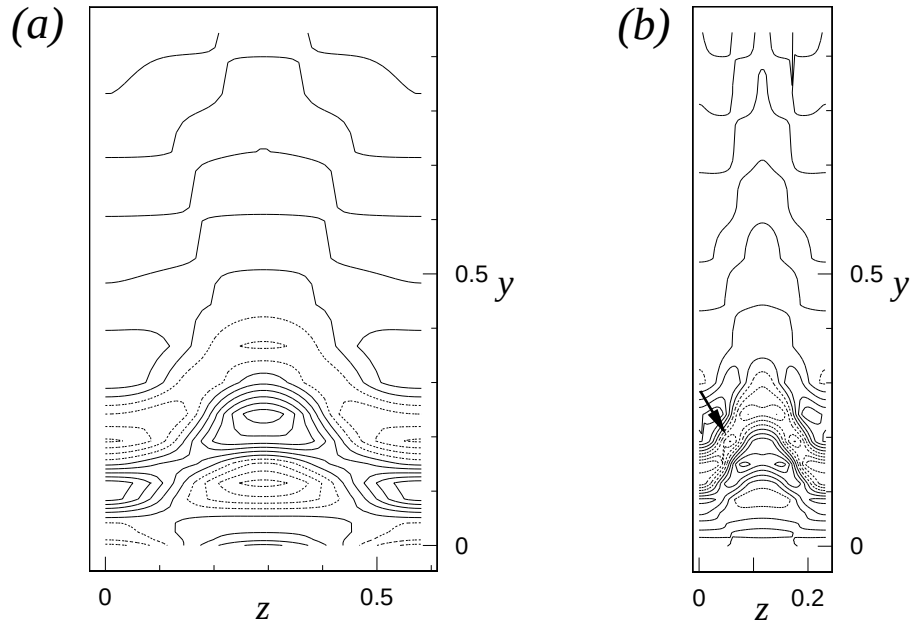

FIGURE 6. Eigenmode $\hat{\omega}_x$ for the streamwise vorticity. (a) $\Delta U = 4.0$, $\gamma = 10.8$, $\alpha = 2.1$ (mode II); and (b) $\Delta U = 4.0$, $\gamma = 27.0$, $\alpha = 11.4$ (mode III). Contour increment is ω'. Negative contours are dotted. Only the real parts of $\hat{\omega}_x$ are shown. In (b) one of the minima, which correspond to the 'arms' in Fig. 4c, is indicated by the arrow.

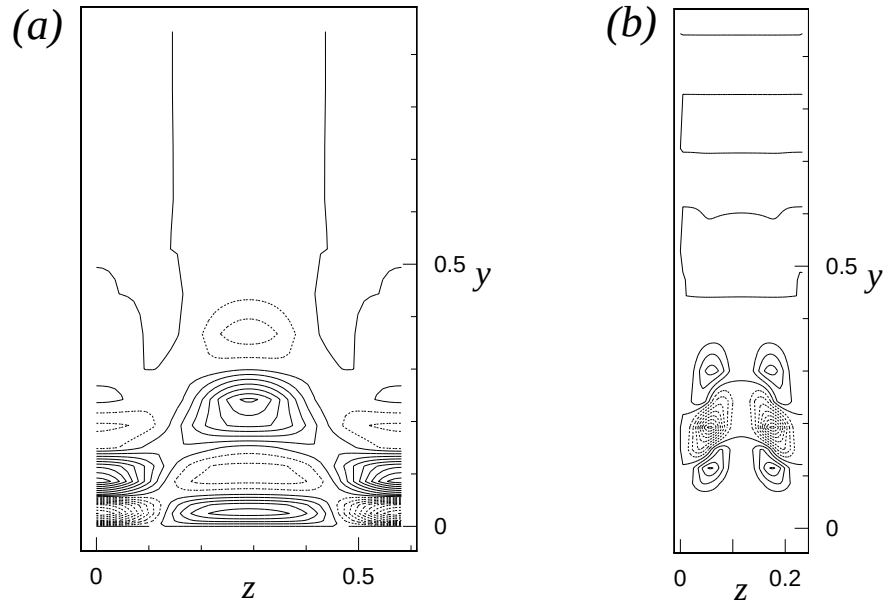

FIGURE 7. Significant production terms for the streamwise vorticity. (a) $-\mathrm{i}\hat{w}(\partial_y U)/\mathrm{Im}(c)$ is shown for $\Delta U = 4.0$, $\gamma = 10.8$, $\alpha = 2.1$ (mode II). (b) $\mathrm{i}\hat{v}(\partial_z U)/\mathrm{Im}(c)$ is shown for $\Delta U = 4.0$, $\gamma = 27.0$, $\alpha = 11.4$ (mode III). Contour increment is $3\omega'$, and negative contours are dotted. Only the real parts are shown.

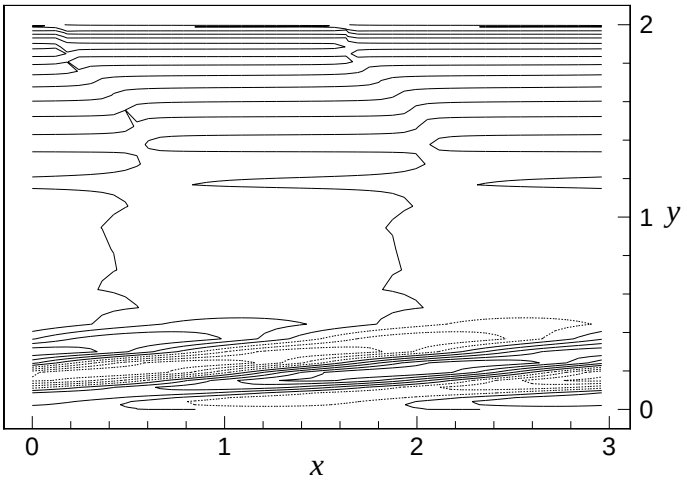

FIGURE 8. Contour plot of the spanwise disturbance velocity on (x, y)-plane for mode II. The slice plane is located at $z = 0.29$, i.e. the centerline of the low-speed streak. Contour increment is v', where v' denotes the RMS value of the velocity vector. Negative contours are dotted.

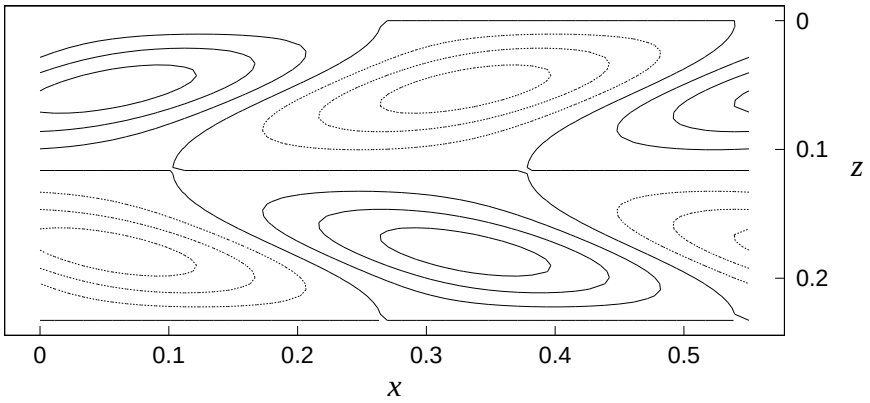

FIGURE 9. Contour plot of the wall-normal disturbance velocity on (x, z)-plane for mode III. The slice plane is located at $y = \frac{1}{6}$, i.e. 30 wall units, where the streak velocity and vorticity attain a maximum. Contour increment is v', where v' denotes the RMS value of the velocity vector. Negative contours are dotted.

bending instability of the streaks similar to a wake-like instability. The eigenmode for the spanwise velocity is inclined from the wall-normal direction towards the streamwise direction under the action of the shearing motion across the wall-normal direction (Fig. 8). The inclined eigenmode for the spanwise velocity directly induces streamwise vorticity as well as wall normal vorticity (see Fig. 10a). The induced

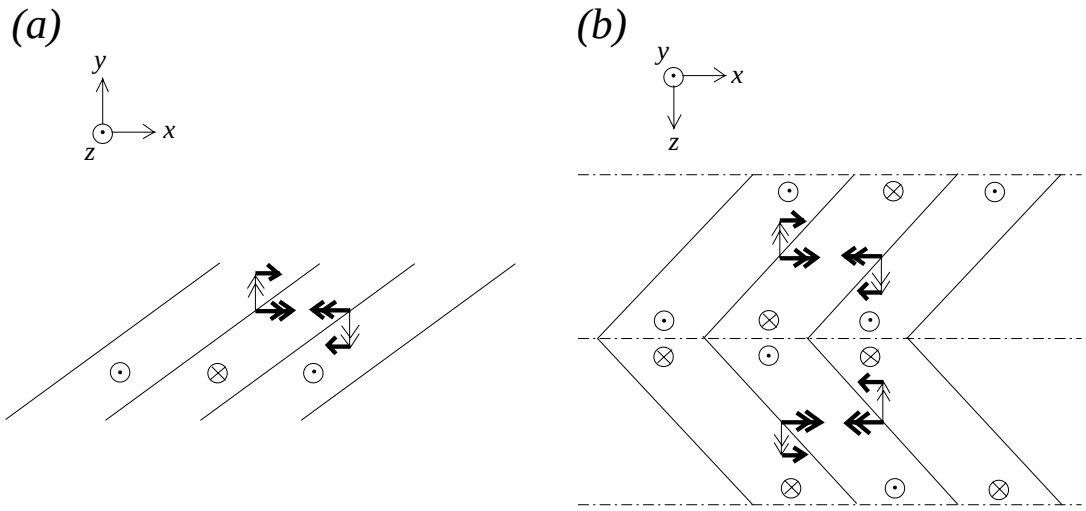

FIGURE 10. Proposed mechanisms of the streamwise vorticity generation for (a) mode II and (b) mode III. Solid lines conceptually show null contours of the disturbance velocity normal to the figure planes, and symbols $\odot$ and $\otimes$ indicate the signs of the velocity component, i.e. coming out of and going in the planes. Thick double arrows denote the induced streamwise vorticity. Thin double arrows denote the induced wall-normal (or spanwise) vorticity in (a) (or in (b)). Thick arrows represent the production of the streamwise vorticity by the vorticity tilting towards the streamwise direction. The dotted-dashed lines in (b) are the centerlines of the low- and high-speed streaks.

wall-normal vorticity is tilted towards the streamwise direction, which then leads to new production of streamwise vorticity. The generated streamwise vorticity, in turn, enhances the spanwise bending of streaks, i.e. the spanwise velocity.

In the case of mode III, on the other hand, one can identify strong localized minima (one of which is indicated by the arrow) of streamwise vorticity situated in between the low- and high-speed streaks in Fig. 6b, which correspond to the 'arms' visible in Fig. 4c. The high vorticity of these minima is apparently produced by the second production term in (15) as the location of the strong minima of production coincides with that of the 'arms' (compare Figs. 7b and 6b).

For mode III, the shearing motion across the spanwise direction is dominant especially between the low- and high-speed streaks. If we examine the order of the disturbance velocity, then we find that the wall-normal velocity much exceeds the spanwise one between the low- and high-speed streaks (the streamwise component is again very small). The eigenmode for the wall-normal velocity is inclined towards the streamwise direction from the spanwise direction by the action of the shear between the low- and high-speed streaks (Fig. 9). The inclined eigenmode for the wall-normal velocity directly induces streamwise vorticity and secondarily produces it through vortex tilting in a manner similar to that found in the case of mode II but with the production taking place essentially in planes parallel to the wall (see

Fig. 10b).

3. Summary and future plans

In this report, we have presented three different instability modes in the base flow composed of a turbulent-channel-type mean flow andsuperimposedstreaks at $Re_\tau = 180$. For $\gamma/Re_\tau < 0.01$, a wall-jet-like instability occurs, and the critical velocity amplitude of streaks is around $\Delta U_c = 1.7$. In the range $0.01 < \gamma/Re_\tau < 0.12$, into which falls the wavelength of 100 wall-units, the critical amplitude is around $\Delta U_c = 3$. In this case, unstable eigenmodes take a form that is inclined towards the streamwise direction from the wall-normal direction, and they directly induce streamwise vorticity. In addition, the streamwise vorticity is secondarily produced on low- and high-speed streaks principally through tilting of the wall-normal disturbance vorticity by the base flow shear across the wall-normal direction. For $\gamma/Re_\tau > 0.12$, on the other hand, the shearing motion between low- and high-speed streaks is dominant so that eigenmodes are oriented in the spanwise direction (with an inclination towards the streamwise direction) rather than in the wall-normal direction. In this case, therefore, the streamwise vorticity is produced between low- and high-speed streaks principally through tilting of the spanwise disturbance vorticity by the base flow shear across the spanwise direction in addition to the direct induction of the streamwise vorticity by inclined eigenmodes. In these latter two cases, the instability is considered to be similar to a wake instability. In these cases, however, the streamwise vorticity is dominant, and it is induced directly through the instability. No two-dimensional instability mechanism can be applied to these two unstable modes. The underlying three-dimensional mechanism is expected to be interpreted directly in terms of the streamwise vorticity.

We are now pursuing an analytical approach to explain the mechanism of the streak instability and the generation of the streamwise vorticity. We are also planning to investigate the effects of a change of boundary conditions on the streak instability in order to get useful information for possible control strategies of near-wall turbulence.

Acknowledgments

The authors are grateful to Dr. Jeffrey Baggett for reviewing the preliminary version of this manuscript. G. K. is supported by the Japanese Ministry of Education, Science and Culture.

REFERENCES

Baggett, J. S. 1996 Non-normal dynamics and applications in hydrodynamic stability. PhD Thesis, Cornell Univ.

Hamilton, J. M., Kim, J. & Waleffe, F. 1995 Regeneration mechanisms of near-wall turbulence structures. *J. Fluid Mech.* **287,** 317-348.

Jiménez, J., Kawahara, G., Pinelli, A. & Uhlmann, M. 1998 Linear stability analysis of turbulent channel flow including porous walls. Tech. Note ETSIA MF-9811, School of Aeronautics, U. Politécnica Madrid, Spain.

Jiménez, J. & Moin, P. 1991 The minimal flow unit in near-wall turbulence. *J. Fluid Mech.* **225,** 213-240.

Jiménez, J. & Pinelli, A. 1998 The autonomous cycle of near-wall turbulence. Submitted to *J. Fluid Mech.*

Reddy, S. C., Schmid, P. J., Baggett, J. S. & Henningson, D. S. 1998 On stability of streamwise streaks and transition thresholds in plane channel flows. *J. Fluid Mech.* **365,** 269-303.

Reynolds, W. C. & Tiederman, W. G. 1967 Stability of turbulent channel, with application to Malkus's theory. *J.Fluid Mech.* **27,** 253-272.

Schoppa, W. & Hussain, F. 1997 Genesis and dynamics of coherent structures in near-wall turbulence: A new look. In *Self-sustaining Mechanisms of Near-Wall Turbulence,* Computational Mechanics Publications, 385-422.

Schoppa, W. & Hussain, F. 1998 Formation of near-wall streamwise vortices by streak instability. *AIAA 98-3000.*

Sendstad, O. & Moin, P. 1992 The near-wall mechanics of three-dimensional boundary layers. *Rep. TF-57,* Thermosciences Division, Dept. Mechanical Engineering, Stanford Univ., Stanford, CA.

Waleffe, F. 1995 Hydrodynamic stability and turbulence: Beyond transients to a self-sustaining process. *Stud. Appl. Math.* **95,** 319-343.

Waleffe, F. 1997 On a self-sustaining process in shear flows. *Phys. Fluids.* **9,** 883-900.

Waleffe, F. & Kim, J. 1997 How streamwise rolls and streaks self-sustain in a shear flow. In *Self-sustaining Mechanisms of Near-Wall Turbulence,* Computational Mechanics Publications, 309-332.

Waleffe, F., Kim, J. & Hamilton, J. M. 1991 On the origin of streaks in turbulent boundary layers. In *Turbulent Shear Flows 8,* Springer, 37-49.